

Cyclic Behavior of Precast Post Tensioned Concrete Shear Wall with and Without Opening

Ahmad Shokoohfar^{a,*}, Peyman Khorshidi^a

^a*Department of Civil Engineering, Qazvin Branch, Islamic Azad University, Qazvin, Iran*

Received 15 August 2021, Accepted 28 April 2022

Abstract

Innovative Precast Post-Tensioned Concrete Shear Wall (PPCSW) comprises two columns as boundary elements and a main precast shear wall. Although, there have been some researches about the cyclic behavior of the PPCSWs, the investigation of the effect of openings in this system has been of less interest. The main purpose of this article is to study the effect of a standard opening on the PPCSWs. The numerical models are prepared for three different heights (3,6, and 9 stories) and their cyclic dissipated energy is compared. The concrete damage plasticity model is applied as constitutive material law. The numerical results demonstrate that by increasing the shear wall's height, the openings become more effective. Therefore, the maximum reduction of dissipated energy belongs to the nine stories shear wall system. And, also the maximum strength reduction due to opening effects is for the nine stories shear wall system. In contrast to the strength and dissipated energy variables, the maximum initial stiffness reduction due to opening effects take place in 3 stories model.

Keywords: Seismic behavior, Concrete shear wall, Precast, Opening, Cyclic behavior.

1.Introduction

Nowadays, the advances in construction methods and increasing the application of rapid construction procedures make the use of precast concrete parts inevitable. Widely use of the precast concrete shear wall arises the necessity of performing more investigation on the seismic performance of their connections.

There are many innovative connections for a precast concrete shear wall. GFRP (Glass Fiber Reinforcing Polymer) bars and SMA (Shaped memory alloys) are applied as vertical connecting bars. The GFRP bars are more efficient under cyclic loads in relation to other connecting bars [1]. In case the steel mild connecting bars are used, the most effective parameter is the overlapping length and some research shows that a code-based overlapping length can be sufficient [2,3]. Huang et. al. applied a combination of shear keys and welding connecting bars to present an innovative way for assembling boundary elements and the main wall part [4]. Precast concrete wall parts can be provided with some greater holes, so the connecting bars can be replaced by the vertical cast-in-place columns. These columns comprise a bundle of longitudinal bars

confined by spiral bars [5]. Some steel bolted plates are also suggested for connection of precast RC walls, however, the efficiency of this method significantly depends on the arrangement of the connection plates and shear keys [6].

In recent years, post-tensioning methods are widely used in precast concrete shear walls. Different arrangements of tendons are used for connecting the prefabricated wall parts. Buddika et. al. considered a uniform post-tensioning tendon accompanying energy dissipated in bars at the level of the foundation. They carried out a series of numerical studies to modify the seismic base shear of the structures including the precast prestressed concrete shear wall (PPCSW) [7]. Experimental studies indicate that higher prestressing forces lead to higher initial stiffness and lower equivalent viscous damping ratios [8]. The comparative study on conventional sleeve connection and the energy dissipating in mild steel bars demonstrate that the cyclic behavior of later one is so higher, and also the dissipated energy of the shear wall system goes higher by increasing the area of the mild steels [9]. Zhangfeng et. al. proved the capabilities of

 *Corresponding Author: Email Address:ahmad.shokoohfar@gmail.com

ABAQUS software to predict the inelastic behavior of post-tensioned shear walls through a series of experimental and numerical studies [10]. A few pieces of research have been performed on the effect of geometric imperfection and openings in the precast post-tensioned system.

This paper presents a numerical study on the cyclic behavior of PPCSWs, with and without openings in different heights. A standard opening with 2 meters height and 3 meters width is considered in the middle of the precast concrete shear wall. Some variables such as dissipated energy, force-displacement envelope and hysteretic force-displacement curves are determined to investigate the cyclic behavior of the models.

2. Analysis Approach

ABAQUS software is selected for the nonlinear analysis of the PPCSWs. The perfect elastoplastic model was considered to define the behavior of steel. The modulus of elasticity, Poisson’s ratio and the yield stress of steel bar were considered as 204000 MPa, 0.3 and 400 MPa, respectively. Also, the tendons’ properties are as follows:

The modulus of elasticity, Poisson’s ratio, the yield stress and the ultimate stress of tendons were considered as 186000 MPa, 0.3, 1520 MPa, and 1750 MPa, respectively. The mechanical properties of concrete were determined based on the concrete test results. The compressive strength, density, the elasticity modulus, and Poisson’s ratio of the concrete were considered to be 35MPa, 2400 kg/m³, 25600 MPa and 0.2, respectively. The concrete damage plasticity (CDP) model is selected to define the nonlinear properties of concrete [11]. To generalize the stress-strain curve, the model developed by Mander et al. [12] is selected (Fig 1).

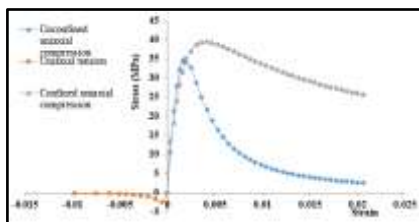


Fig. 1. Stress-strain curve of the concrete.

The eight-node reduced integrated cubic elements C3D8R were selected for the concrete parts. The dual-node 3D truss element T3D2 was utilized for reinforcement bars and tendons. The mesh size of

the elements was determined about 142 mm based on the test results. The data needed for forming yield surface in the CDP model are presented in Table. 1.

Table 1
Plasticity parameters of CDP [11]

ψ	Eccentricity	f	k	Viscosity parameter
31	0.1	1.16	0.667	0.001

In the Table 1, ψ is the dilation angle, f is ratio of initial biaxial compressive yield stress to initial biaxial compressive yield stress $\sigma_{bo} / \sigma_{co}$, and k is the ratio of second variable of stress on deviated stress axis (q_{CM}) to the same value on deviated stress axis (q_{TM}). The second variable of stress can be expressed as:

$$I_2 = \sigma_{11}\sigma_{23} + \sigma_{22}\sigma_{33} + \sigma_{11}\sigma_{33} - \sigma_{12}^2 - \sigma_{23}^2 - \sigma_{31}^2 \quad (1)$$

Where, σ_{ii} is the stress components. Figure 2 indicate the three-dimensional yield stress surface on the deviated stress planes.

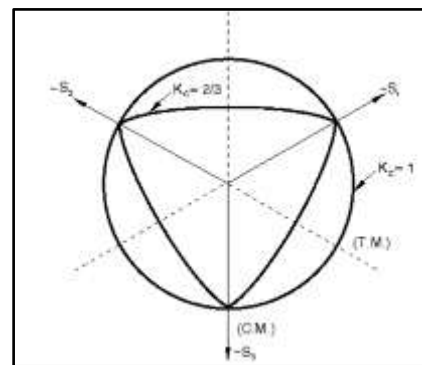


Fig. 2. Three-dimensional yield stress surface on the deviated stress planes [11]

3. Finite Element Model Properties

Generally, six models are dimensioned and created using Etabs software based on the ACI-318 [13] and the design algorithm presented by Todut et. al. [14]. Models are prepared in 3,6 and 9 stories and the story dimension is assumed to be 4000 (h) to 5000 (w). A standard opening with the dimension of 2000 (h) and 3000 (w) is considered at the middle of the shear wall panel. All degrees of freedom are restrained for the nodes located at the bottom of the model. The connecting tendons are 4,8, and 12 numbers of 1/4" cable for the models with 3,6, and

nine stories respectively. The loading protocol is presented in Fig. 3, which is extracted from FEMA 461 [15] and the target displacements are determined based on FEMA 356 [16]. The ultimate target displacement is obtained as 81.16 mm, 169.3 mm, and 309.5 mm for the structure with 3, 6, and 9 stories, respectively.

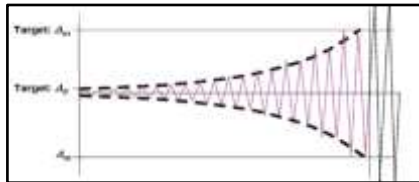


Fig. 3. Lateral loading protocol

4.Verification of Analysis Method

The mesh size and analysis steps should be verified using experimental results. In the current study, an experimental work carried out by Todut et. al. is selected to validate the numerical modeling procedure [14]. A lateral displacement of about 12.9 mm and an axially compressive force of about 100 kN are considered and imposed respectively based on the experimental procedure. The sample details are presented in Fig. 4.

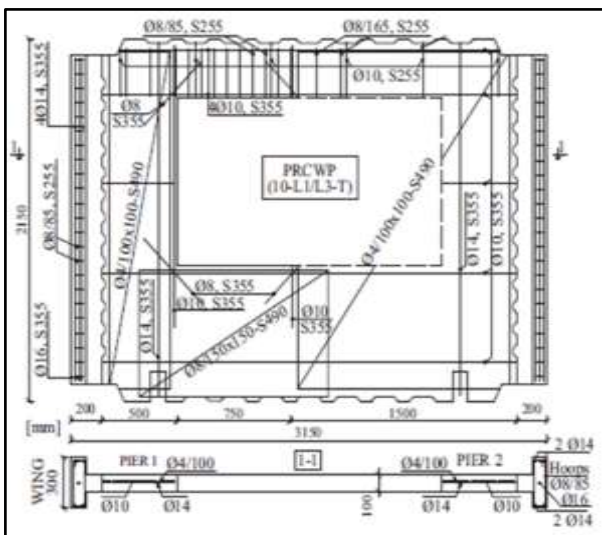


Fig. 4. Drawing details of specimen [14]

Fig. 5 illustrates the results after the sample is loaded in both the numerical and the experimental cases. The ABAQUS software gives a fairly good prediction about the stress distribution of the real case. Also, in Fig .6, diagrams show a good agreement between ABAQUS results and the experimental test results.

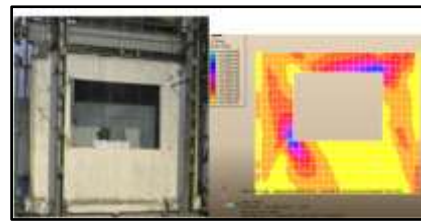


Fig. 4. Drawing details of specimen [14]

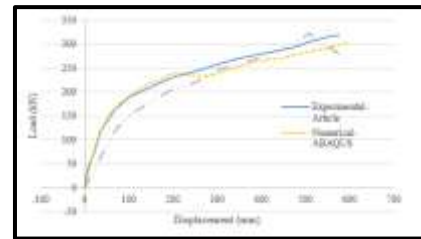


Fig. 6. Comparison of experimental and numerical result

5.Results and Discussion

The numerical results are displayed for the force-displacement envelope, energy dissipation, and hysteretic curves. As illustrated in Fig. 7, although, the stress contour in the model with openings is localized around the openings, the maximum stress is in a similar location as the model without any openings. These circumstances are repeated in other models.

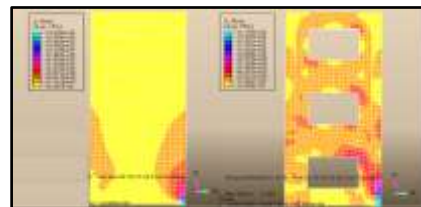


Fig. 7. Comparison of the stress contour in the model with and without openings; (Unit of stress contour: MPa)

Fig. 8 displays hysteretic force displacement curves for models with 6 stories. The envelope and energy dissipated curves are extracted from the hysteretic curves. The hysteretic curve goes thinner by increasing the PPCS height. The lateral force-displacement curves present the main characteristics of the models such as initial stiffness, ductility and strength capacity. Fig. 9 compares all models' results. Naturally, the slender models show more ductility despite the lower stiffness. The stiffness reduction percent due to opening effects is increased by decreasing the model's height. The stiffness reduction is about 27%, 18%, and 15% for 3,6, and 9

stories, respectively. The opening has fewer effects on the ductility of the models.

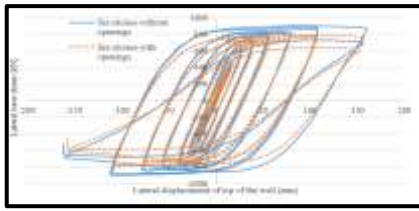


Fig. 8. Hysteretic force-displacement results for six stories model

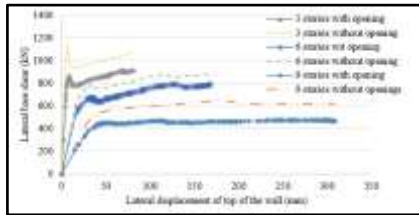


Fig. 9. Comparison of the stress contour in the model with and without openings

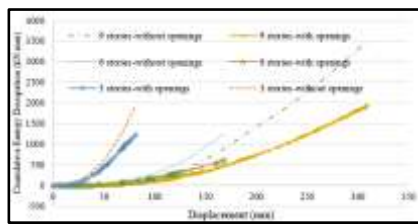


Fig. 10. Comparison of cumulative energy in the models, with and without openings

The most notable parameter to understand the cyclic behavior of a structure is dissipated energy. Fig. 10 displays cumulative dissipated energy curves for models with and without openings. As it can be inferred from Fig. 10, the difference between the cases with openings and without openings is more apparent at the last loops of the hysteretic curves. Hence, the effects of the openings are more distinctive in higher ranges of lateral displacement. In fact, the openings are more effective in the inelastic domain of structural behavior.

6. Conclusions

The cyclic behavior of precast prestressed concrete shear wall (PPCSW) was investigated through numerical studies of the models with different heights, with and without openings. The models are analyzed under a cyclic loading protocol based on FEMA 461 [15]. The following conclusions can be drawn from the numerical results of considered 6 cases:

- 1- The initial stiffness reduction due to opening effects is decreased in all models.
- 2- The strength capacity reduction due to opening effects is amplified by increasing the lateral displacement. The average value of strength reduction is about, 12.43%, 16.33%, and 22.71% for the 3, 6, and 9 stories, respectively. The strength reduction is increased in all models.
- 3- The opening effects reduce cumulative energy dissipation, particularly, in inelastic domains of lateral displacements. This reduction is amplified by increasing the lateral displacement. The average value of strength reduction is about 29.13%, 34.34%, and 43.56% for the 3, 6, and 9 stories, respectively. The energy dissipation reduction is increased in all models.

A standard opening like a window can reduce the efficiency of the PPCSW models. The worst results belong to 9 stories cases, therefore, by increasing the number of stories the opening effects become more influential. According to analyses results the some suggestions can be offered for future studies; A comprehensive parametric study can be performed on the effect of different arrangement of strengthening rebars laid along openings edges, and also, the current parametric study can be continued over high-rise buildings.

References

- [1] Tolou Kian, M. J., & Cruz-Noguez, C. (2018). Reinforced concrete shear walls detailed with innovative materials: seismic performance. *Journal of Composites for Construction*, 22(6), 04018052.
- [2] Gu, Q., Dong, G., Wang, X., Jiang, H., & Peng, S. (2019). Research on pseudo-static cyclic tests of precast concrete shear walls with vertical rebar lapping in grout-filled constrained hole. *Engineering Structures*, 189, 396-410.
- [3] Molaei Manzar, A., & Aghabarati, H. (2016). Evaluation of the Effect of Connection between RC Shear Wall and Steel Moment Frame on Seismic Performance and Reduction Factor in Dual Systems. *Journal of Structural Engineering and Geo-Techniques*, 6(2), 31-39.
- [4] Huang, W., Zhang, M., & Yang, Z. (2018). A comparative study on seismic performance of precast shear walls designed with different variables. *KSCE Journal of Civil Engineering*, 22(12), 4955-4963.
- [5] Chen, Y., Zhang, Q., Feng, J., & Zhang, Z. (2019). Experimental study on shear resistance of precast RC shear walls with novel bundled connections. *Journal of Earthquake and Tsunami*, 13(03n04),

1940002.

- [6] Shen, S. D., Cui, Y., Pan, P., Gong, R. H., Miao, Q. S., & Li, W. F. (2019). Experimental study of RC prefabricated shear walls with shear keys affected by a slotted floor slab. *Journal of Aerospace Engineering*, 32(3), 04019013.
- [7] Buddika, H. S., & Wijeyewickrema, A. C. (2018). Seismic shear forces in post-tensioned hybrid precast concrete walls. *Journal of Structural Engineering*, 144(7), 04018086.
- [8] Twigden, K. M., Sritharan, S., & Henry, R. S. (2017). Cyclic testing of unbonded post-tensioned concrete wall systems with and without supplemental damping. *Engineering Structures*, 140, 406-420.
- [9] Gu, A., Zhou, Y., Xiao, Y., Li, Q., & Qu, G. (2019). Experimental study and parameter analysis on the seismic performance of self-centering hybrid reinforced concrete shear walls. *Soil Dynamics and Earthquake Engineering*, 116, 409-420.
- [10] Zhu, Z., & Guo, Z. (2017). Experimental study on emulative hybrid precast concrete shear walls. *KSCE Journal of Civil Engineering*, 21(1), 329-338.
- [11] D Simulia Inc. ABAQUS/ user's guide, Version 6.21 (2021). <http://abaqus.software.polimi.it/v2021/> (2021).
- [12] Mander, J. B., Priestley, M. J., & Park, R. (1988). Theoretical stress-strain model for confined concrete. *Journal of structural engineering*, 114(8), 1804-1826.
- [13] ACI Committee. (2019). Building code requirements for structural concrete (ACI 318-19) and commentary. American Concrete Institute.
- [14] Todut, C., Dan, D., & Stoian, V. (2014). Theoretical and experimental study on precast reinforced concrete wall panels subjected to shear force. *Engineering Structures*, 80, 323-338.
- [15] FEMA 461 (2007). Interim Testing Protocols for Determining the Seismic Performance Characteristics of Structural and Nonstructural Components, APPLIED TECHNOLOGY COUNCIL 201 Redwood Shores Parkway, Suite 240 Redwood City, California.
- [16] FEMA 356 (2000). Pre-standard and commentary for the seismic rehabilitation of buildings, American society of Civil Engineers, Reston, Virginia.